Stem Cell Reports
Article

ISSCR

OPEN ACCESS

Astrocytic Calcium Waves Signal Brain Injury to Neural Stem and Progenitor Cells

Anna Kraft,[1] Eduardo Rosales Jubal,[2,3] Ruth von Laer,[1] Claudia Döring,[4] Adriana Rocha,[5] Moyo Grebbin,[1] Martin Zenke,[6] Helmut Kettenmann,[5] Albrecht Stroh,[2] and Stefan Momma[1,*]

[1]Institute of Neurology (Edinger Institute), Frankfurt University Medical School Frankfurt, 60528 Frankfurt, Germany
[2]Focus Program Translational Neuroscience (FTN) and Institute for Microscopic Anatomy and Neurobiology, Johannes Gutenberg University Mainz, 55128 Mainz, Germany
[3]Faculty of Psychology, Diego Portales University, Santiago, Chile
[4]Dr. Senckenberg Institute of Pathology, Frankfurt University Medical School, German Cancer Consortium (DKTK), German Cancer Research Center (DKFZ), 60528 Frankfurt, Germany
[5]Cellular Neuroscience, Max Delbrück Centre for Molecular Medicine (MDC) in the Helmholtz Society, 13092 Berlin, Germany
[6]Institute for Biomedical Engineering, Department of Cell Biology, RWTH Aachen University Medical School, 52074 Aachen, Germany
*Correspondence: stefan.momma@kgu.de
http://dx.doi.org/10.1016/j.stemcr.2017.01.009

SUMMARY

Brain injuries, such as stroke or trauma, induce neural stem cells in the subventricular zone (SVZ) to a neurogenic response. Very little is known about the molecular cues that signal tissue damage, even over large distances, to the SVZ. Based on our analysis of gene expression patterns in the SVZ, 48 hr after an ischemic lesion caused by middle cerebral artery occlusion, we hypothesized that the presence of an injury might be transmitted by an astrocytic traveling calcium wave rather than by diffusible factors or hypoxia. Using a newly established in vitro system we show that calcium waves induced in an astrocytic monolayer spread to neural stem and progenitor cells and increase their self-renewal as well as migratory behavior. These changes are due to an upregulation of the Notch signaling pathway. This introduces the concept of propagating astrocytic calcium waves transmitting brain injury signals over long distances.

INTRODUCTION

Different types of brain injuries, such as ischemia or trauma, have been reported to influence adult neurogenesis in the two stem cell niches of the adult brain (Arvidsson et al., 2002; Takasawa et al., 2002). In the subventricular zone (SVZ), these injuries lead to enhanced proliferation and migration of neuroblasts, not only to the olfactory bulb but also toward the damaged area. Interestingly, brain tumors, such as glioblastoma, also stimulate the migration of immature precursor cells toward the tumor mass, as these cells can be found at the tumor edge (Chirasani et al., 2010; Glass et al., 2005). A neurogenic response to pathologies such as stroke (Jin et al., 2006; Macas et al., 2006), Huntington disease (Curtis et al., 2003), epilepsy (Crespel et al., 2005), or brain tumors (Macas et al., 2014) has also been reported in adult human brains. These results have fueled hope of using the activation of endogenous neural stem cells in response to injury as an additional strategy for the treatment of neurological diseases (Lindvall and Kokaia, 2006). Recent findings of ongoing neurogenesis in the adult human striatum and hippocampus (Ernst et al., 2014; Spalding et al., 2013) have lent further support to this prospect. Multiple factors and signaling pathways have been described as playing a role in the injury reaction of the SVZ. Among the most prominent are the Notch signaling pathway and the SDF-1α ligand and its receptor CXCR4 (Imitola et al., 2004). Notch is reported to upregulate the proliferation and differentiation of cells in the SVZ in a stroke model, while SDF-1α has been shown to influence the direction of migration toward injured regions. However, the question of which signals, emanating from the injury site, are responsible for initiating the injury reaction of neural stem cells (NSCs) in the SVZ has received little attention. Such a signal would require the fulfillment of several criteria: Firstly, it has to be transmitted quickly, as changes in gene expression in the murine SVZ occur as early as 4 hr after the lesion (Wang et al., 2009b). Secondly, the signal must be relayed over relatively large distances, arguing against diffusible factors. Thirdly, the signal must be spatially orientated, as changes in the SVZ largely occur in the hemisphere, ipsilateral but not contralateral to the injury. Finally, it must be self-sustainable. By analyzing gene expression patterns in the SVZ 48 hr after permanent middle cerebral artery occlusion (MCAO) in mice, we found a prominent change in the expression levels of calcium-binding proteins based on gene ontology (GO) classification, indicating a possible role of calcium signaling in the initiation of the injury reaction. Together with other observations, this led us to the hypothesis that information about an injury induced by stroke may be transmitted to the SVZ by traveling astrocytic calcium waves, transient increases in intracellular calcium that transmit to adjacent non-stimulated astrocytes and thereby spread over long distances (Scemes and Giaume, 2006). Calcium waves display a wide range of physiological

functions in the brain. In development, calcium increases have been shown to modulate cell division, neuronal differentiation, and migration (Owens and Kriegstein, 1998; Stroh et al., 2011). More recently, it has been shown that postnatal neural stem and progenitor cells (NSPCs) in the SVZ can communicate with astrocytes via gap junction-mediated calcium waves (Lacar et al., 2011), and calcium signaling in the adult SVZ has been shown to modulate blood vessel dilation (Lacar et al., 2012). However, to the best of our knowledge, a mechanism by which distant signals from injuries can be relayed by astrocytic networks to NSCs has not been described.

To study the activation of NSCs by astrocytic calcium waves in a system with reduced complexity, we developed a co-culture system to allow this signaling to be investigated in isolation. Functionally, NSCs stimulated by an astrocytic calcium wave increase their rate of self-renewal as well as their migratory capacity. The Notch pathway has been implicated in many aspects of stroke-induced neurogenesis (Carlén et al., 2009; Felling et al., 2006; Kawai et al., 2005; Wang et al., 2009a). Accordingly, we observed an early and transient upregulation of the Notch target gene *Hes1* in culture and organotypic slices. Inhibition of the Notch pathway with a γ-secretase inhibitor abolished the increased migration potential. In sum, we propose that propagating calcium waves are a major contributor to the initiation of the injury response of SVZ NSCs after ischemia.

RESULTS

Cellular and Gene Expression Changes in the SVZ 48 hr after MCAO

To analyze changes in gene expression with regard to the possible initiation of the injury reaction in the SVZ after stroke, we performed Affymetrix chip expression analysis on SVZ tissue dissected out 48 hr after permanent MCAO. SVZ tissue from animals undergoing sham surgery served as control (n = 3 independent experiments, 15–20 animals per experiment) (Figure 1A). Brains with the tissue damage extending to the SVZ were excluded from our analysis to minimize confounding factors such as dead tissue or infiltrating blood cells. We further analyzed tissue sections from the same groups of animals to control for changes in cell composition due to the possible influx of leukocytes. We did not observe any noticeable changes in or around the SVZ in our injury model compared with the contralateral hemisphere or sham controls, with respect to the presence of cells expressing CD45 or the microglia marker Iba1 (Figures 1B, 1C, and S1A–S1C). In analyzing gene expression we found a significant upregulation of genes involved in cell proliferation, cell migration, or cell division. Interestingly, genes for calcium-binding proteins were also highly upregulated in MCAO samples (Figures 1D–1F). We did not find a signature consistent with a hypoxic response. This pattern, together with other considerations mentioned above, led us to the hypothesis that signaling of a distant injury to the SVZ could be mediated by astrocytic calcium waves.

Spatiotemporal Characteristics of Calcium Wave Dynamics in Astrocytes Differentiated from NSCs

To test the concept of a signal relay by astrocytic calcium waves to NSCs without confounding neuronal processes such as spreading depression, we sought to establish an in vitro model. To this end, we differentiated astrocytes from NSCs derived from the SVZ of adult C57/BL6 mice. NSCs can be efficiently differentiated into astrocytes by the addition of ciliary neurotrophic factor (CNTF) and serum to the culture medium (Johe et al., 1996). Differentiation of NSCs with 10 ng/mL CNTF led to >98% differentiation of cells into glial fibrillary acidic protein (GFAP)-positive astrocytes. Virtually no class III β-tubulin (Tuj1)-positive neuronal progenitor cells could be detected. To measure calcium dynamics in the culture, we loaded the astrocytic monolayer with one or other of the fluorescent calcium indicators Fluo4-AM and Oregon Green 1 (OGB1), prior to mechanical injury and subsequent analysis (Figure 2A). A mechanical injury was induced by cutting into the astrocyte monolayer with a scalpel or a 10-μL pipette tip, and subsequent changes in fluorescence intensity over time were analyzed using high-frequency microscopic imaging (19–23 frames/s). We observed a traveling calcium wave starting from the injury site (Figure 2B) and recruiting the entire astrocytic monolayer in the tissue culture well. The wave front appeared as a direct positive relationship between the Euclidean distance from the mechanical injury site and the time delay of the peak fluorescence of the cells' somata with respect to the time point of injury (Figure 2C). The velocity of the wave corresponded to the slope of the best-fitting line. In the astrocyte culture, we observed a velocity of 0.014 mm/s. In the neurosphere-astrocyte co-culture a similar wave was observed, which invaded the neurosphere with a velocity of 0.022 mm/s (Figures 2D–2H). We demonstrated that linear fitting of the relationship between time after injury and peak fluorescence explained a large portion of the variance in both cultures; 90% for the astrocytic (adjusted R^2 = 0.9022) and 78.2% for neurosphere-astrocyte (adjusted R^2 = 0.782) cultures.

Calcium Waves Require Intracellular and Extracellular Calcium and Can Be Mediated by ATP and Gap Junctions

Astrocytic calcium wave propagation can have various underlying physiological processes, depending on the brain

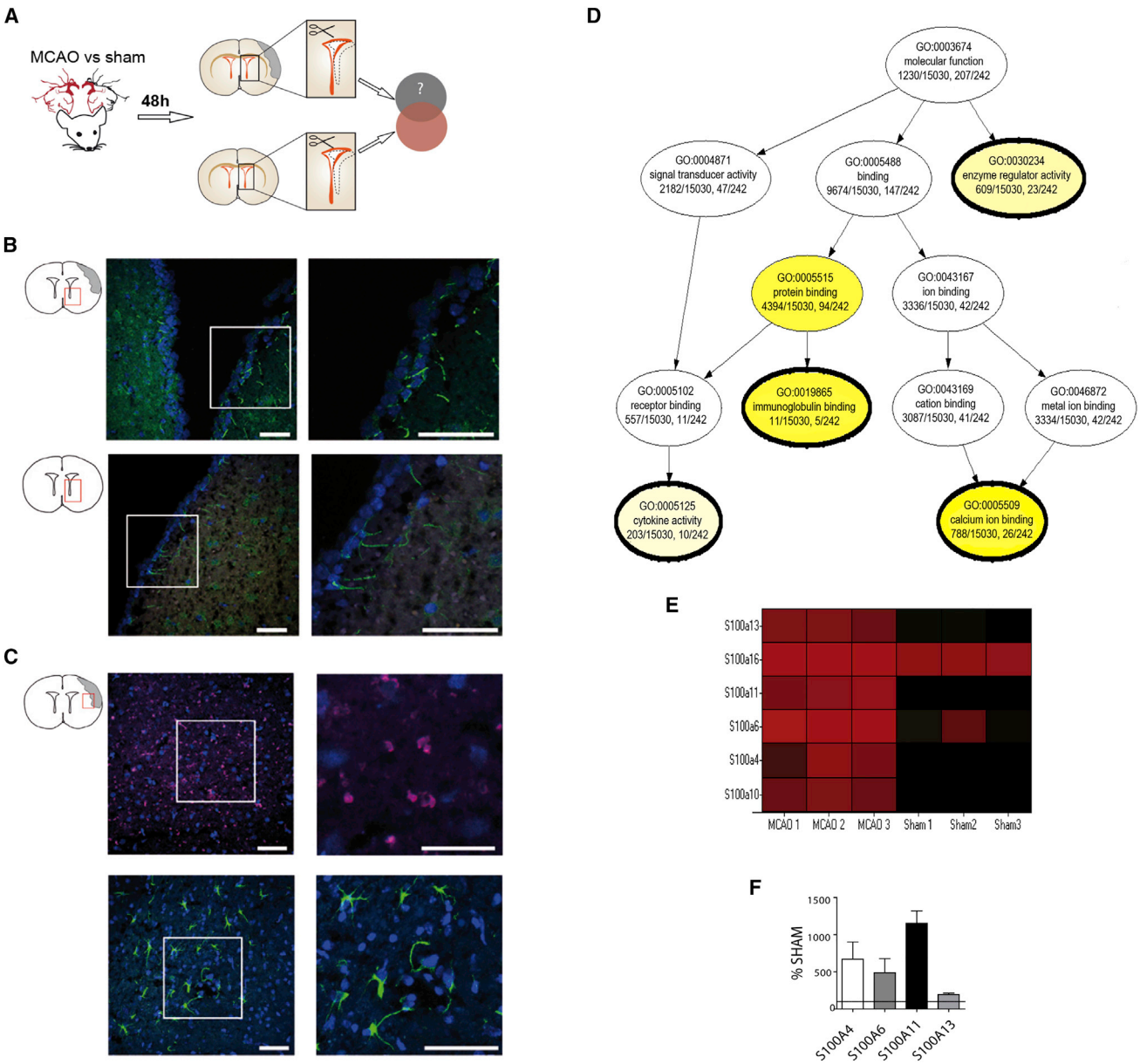

Figure 1. Gene Expression Analysis of the SVZ in Response to an MCAO after 48 hr

(A–C) Experimental scheme. A group of mice underwent surgery, permanently occluding the middle cerebral artery. In the control group, sham surgery was performed without occlusion. Mice were killed 48 hr later and the SVZ dissected out and collected (three separate preparations from 15–20 mice for each group). The composition of the SVZ did not change regarding the influx of blood cells or microglia measured by expression of *CD45* and *Iba1* (B). In contrast, we observed high numbers of marker-positive cells in the penumbra site at injury (C). Scale bars, 100 μm.

(D–F) GO term analysis (D) revealed a strong upregulation of genes belonging to the calcium ion-binding cluster. Absolute expression levels of selected calcium ion-binding proteins are shown as a heatmap, with an increase in expression in the MCAO group (E). Expression levels were confirmed by qPCR analysis (F). Relative expression levels were set at a value of 100% for sham controls. The reaction was performed in triplicate; results are depicted as mean ± SD.

region or type of injury. Therefore, we wanted to characterize the mechanism for calcium wave formation in our cultivated NSC-derived astrocytes. A representative image of a normal calcium wave, arising after a cut into the astrocyte monolayer, is depicted in Figure 3A. Following the addition of 10 nM thapsigargin or 50 μM cyclopiazonic

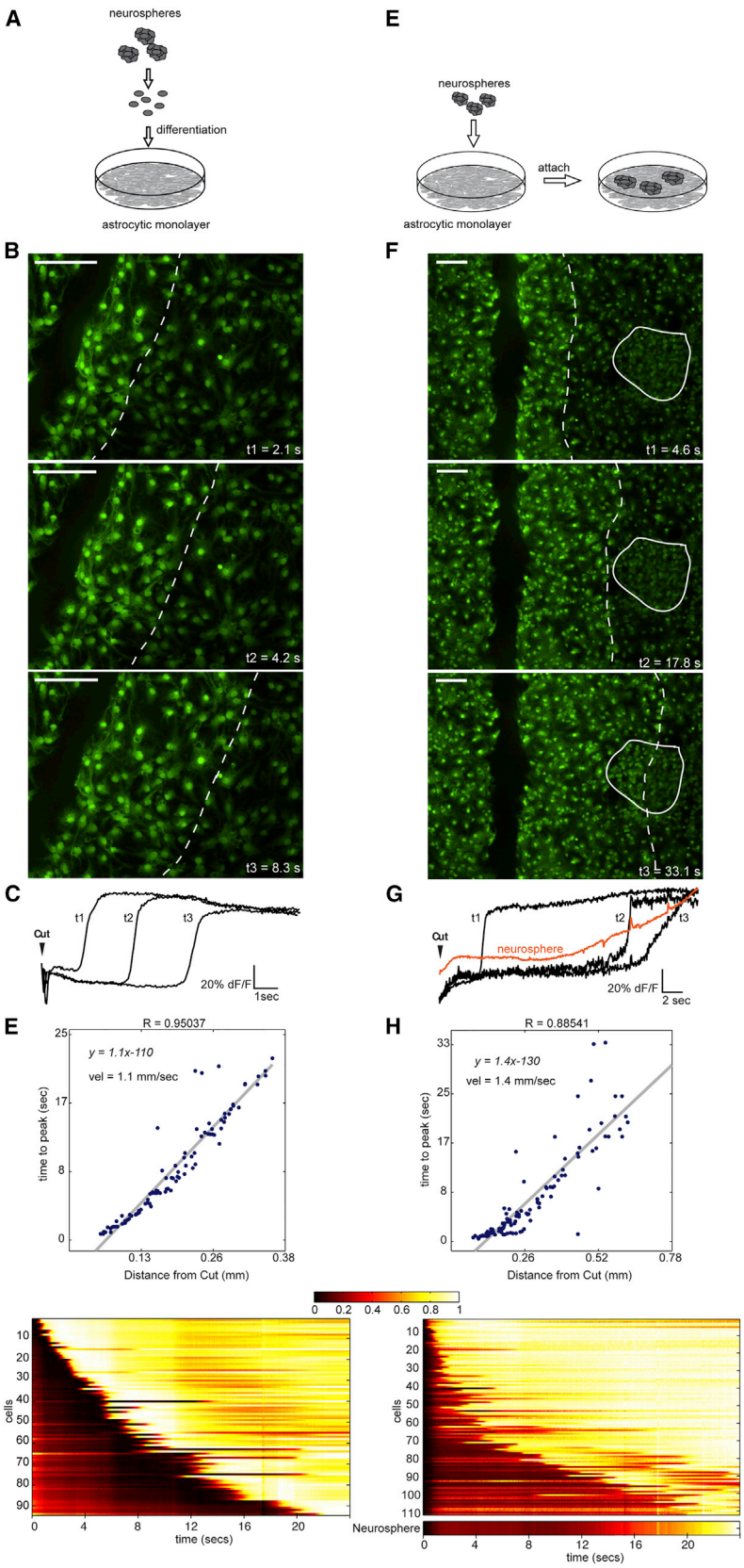

Figure 2. Analysis of Calcium Wave Dynamics

(A) Schematic of the generation of the astrocyte monolayer differentiated from NSCs.

(B) Induction of a bidirectional calcium wave upon mechanical injury. Epifluorescence images of an astrocytic monolayer stained with the fluorescent calcium indicator OGB1 were recorded at 19–23 Hz at different time points after the cut. Dashed lines represent the wave front. Scale bars, 100 μm.

(C) Time series of the fluorescence emission of a cell at the wave front at a given time point.

(D and H) Linear relationship between distance from cut and time to fluorescence peak. Top: linear regression reveals that a linear fit explains a high percentage of variance in both experiments. The slope of the best-fitting line represents the velocity of the calcium wave. Bottom: heatmap depicting the traveling calcium wave. When cells are sorted by their distance to the injury site, the wave dynamic is unveiled. Fluorescence values were normalized.

(E) Schematic of the seeding of neurospheres on the astrocytic monolayer.

(F) Calcium wave induction upon mechanical injury in an astrocyte-neurosphere co-culture. Individual raw images at different time points after the cut. Dashed lines represent the wave front and the area bordered by the solid line indicates the location of a neurosphere. Scale bars, 100 μm.

(G) Time series of the fluorescence emission of a cell at the wave front at a given time point.

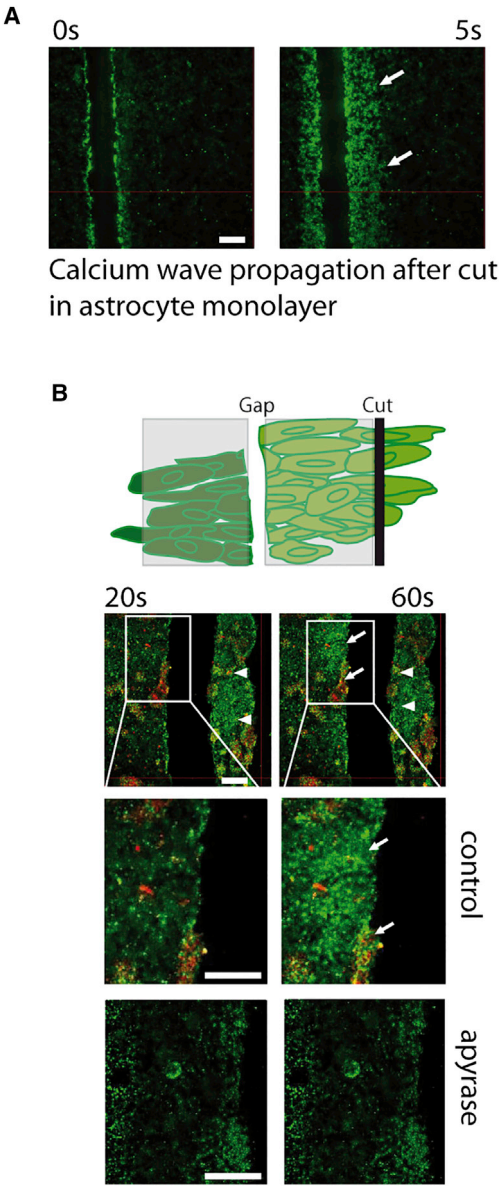

Figure 3. Parameters of Calcium Wave Propagation

A cut into an astrocytic monolayer leads to the spreading of a calcium wave over time.

(A) Still images from movie records, showing an increased fluorescence in astrocytes stained with 5 μM Fluo-4AM, reflecting elevated intracellular calcium levels. Arrows indicate the wavefront. Scale bar, 100 μm.

(B) Experimental setup to test for diffusible signal to carry an astrocytic calcium wave over a gap. Initiation of a calcium wave on the other side of the gap after a time delay in control experiments (upper two panels) and blockage of the transfer after addition of the ATP-degrading enzyme apyrase to the culture medium (lower two panels). Arrows point to neurospheres, arrowheads to the wavefront. Scale bars, 100 μm.

acid (CPA), which deplete calcium from internal stores, no calcium waves could be observed after a cut, underlining the necessity of internal calcium stores for wave propagation (Figures S2A–S2C). Given the potential toxicity of thapsigargin and CPA, we tested their effect on astrocytic cell death and found no increase under the conditions used (Figure S2F). Intracellular calcium is stored in the ER and calcium released from this store is either inositol triphosphate (IP_3) dependent or ryanodine receptor dependent. To determine which stores are involved in wave formation, we treated cells with high (50 μM) or low (20 μM) concentrations of 2-aminoethoxydiphenyl borate (2-ABP), known to block IP_3-dependent and ryanodine-dependent calcium release, respectively. While a low concentration of 2-ABP did not have any effect, a high concentration abolished the formation of calcium waves, comparable with thapsigargin treatment (Figures S2D and S2E). Thus, calcium waves arising after an in vitro injury rely on intracellular calcium stores in an IP_3-dependent manner. To test whether extracellular calcium is required, we added 2 mM EGTA, a highly sensitive non-cell permeable calcium chelator, to the culture medium. Under this condition, calcium waves were abolished (Figure S2H). Astrocytes are highly connected through gap junctions, ion-permissive cell-cell connections that have been reported to play a crucial role in astrocytic calcium wave formation and propagation (Boitano et al., 1992; Cotrina et al., 1998). To test whether calcium waves in the established in vitro system were gap junction dependent, we closed gap junctions either by addition of 50 μM carbenoxolone or by reducing the pH to 6.5; both abolished calcium wave formation (Figures S2G and S2I). To test whether ER stores were completely depleted after thapsigargin and CPA treatment, we additionally added ATP in a calcium-free medium and did not observe the initiation of a calcium wave (Figure S2G). As an alternative route, many diffusible factors can lead to calcium elevation in different cell types, among them ATP (Guthrie et al., 1999). To assess whether calcium waves can be propagated by diffusible factors, we performed calcium-imaging experiments to investigate whether calcium waves could traverse a gap in the astrocytic monolayer. A cell-free gap was created in an astrocytic monolayer by scratching with a pipette tip, following resting time for the arising wave to decay. In the next step, the astrocytic monolayer was cut again at some distance to the initial gap (scheme in Figure 3B). Following the cut, a calcium wave could be seen to emerge from the other side of the gap with some delay (Figure 3B, upper panel). To determine whether ATP was the diffusible factor required for traversing the gap, we added apyrase, an ATP-degrading enzyme, to the culture medium. Under this condition, the calcium wave traveled only to the gap but did not cross it (Figure 3B, lower panel). In conclusion, calcium

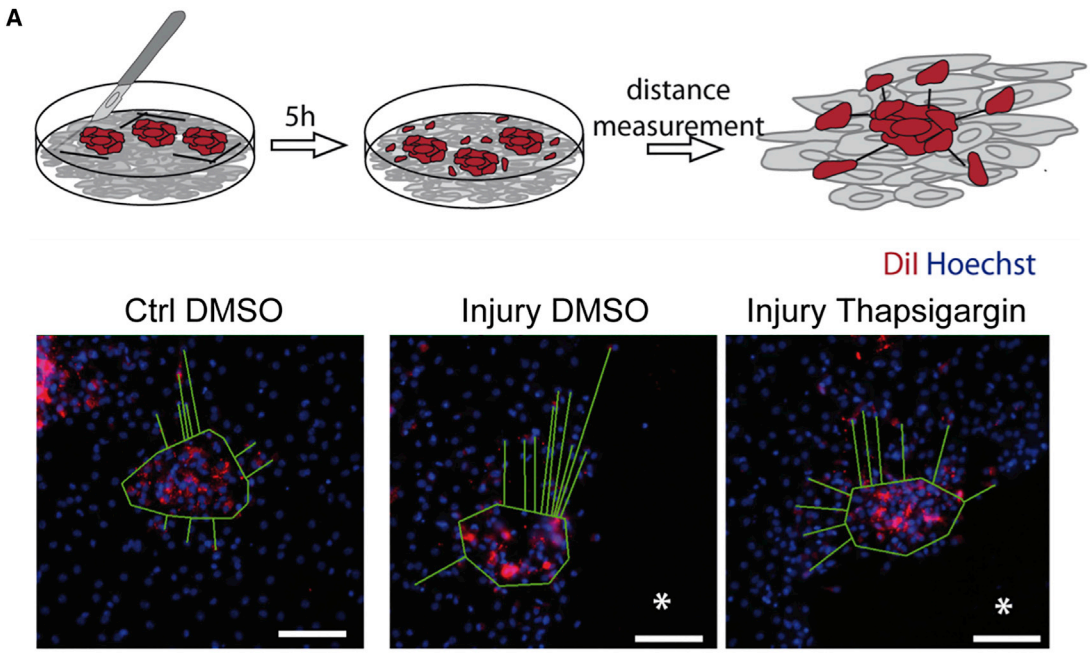

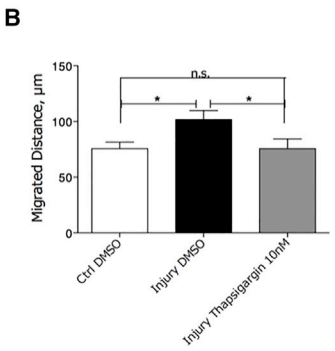

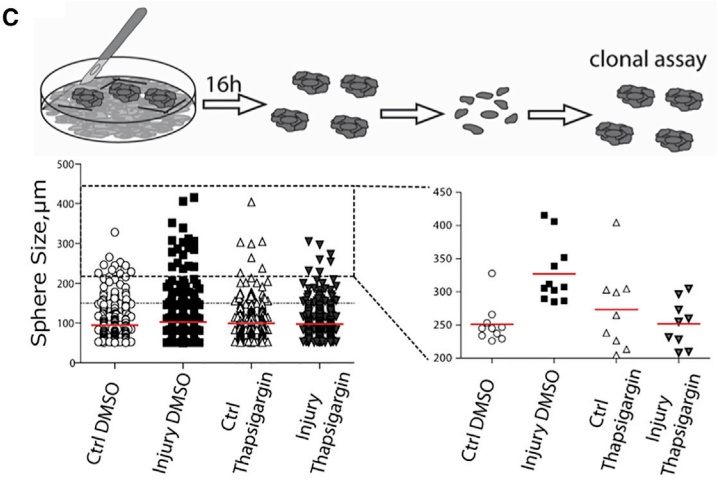

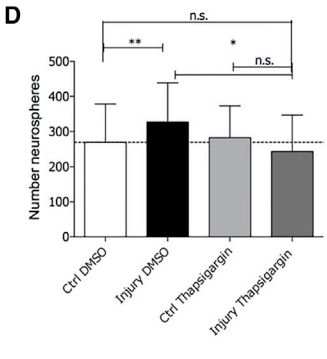

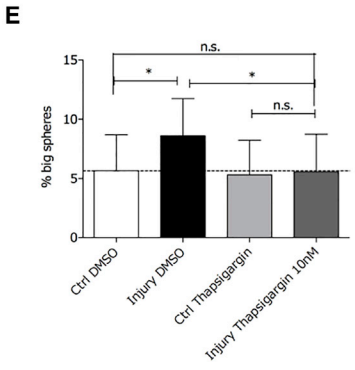

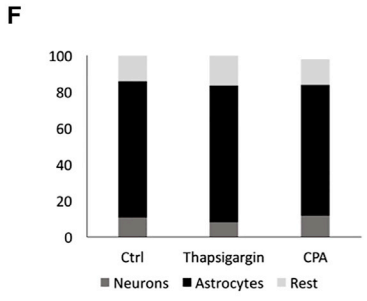

(legend on next page)

waves in vitro require internal cellular calcium stores and calcium release in an IP_3-dependent manner as well as calcium from the extracellular space. Furthermore, gap junction connections and ATP mediate wave propagation between the astrocytes.

Astrocytic Calcium Waves Spread to Co-cultured NSPCs, Eliciting Increased Self-Renewal and Migratory Capacity

To study the effects of astrocytic calcium waves on NSPCs, we pre-labeled neurospheres with the lipophilic dye DiI and seeded them onto an astrocyte monolayer as described above. As a negative control, astrocytes were treated with thapsigargin prior to the attachment of the neurospheres, thereby irreversibly depleting internal calcium stores and abolishing calcium waves in astrocytes alone. This experimental setup was used to assess the effect of calcium waves on changes in the migratory capacity of NSPCs, in line with the observation of a changed migration pattern toward the site of an injury (Arvidsson et al., 2002). Five hours after cutting into the astrocyte layer, the distances of the ten labeled cells that had migrated the furthest beyond the sphere border were measured (Figure 4A). In the thapsigargin-treated sample, the average migration distance was unchanged from that of the uninjured control (average of 75 μm for both conditions, ±5 μm and ±3.4 μm, respectively). However, in the untreated sample the migration distance significantly increased to 101 μm (±4.6 μm) (Figure 4B). Notably, morphological differences between the control or thapsigargin samples versus the injury sample could be observed. The spheres in the thapsigargin and control samples were more condensed and could be easily discriminated from the astrocytic monolayer. In contrast, spheres in the DMSO sample did not exhibit clear boundaries. Next, we assessed the effect of a calcium wave on proliferation and self-renewal of NSCs. For self-renewal, we allowed DiI-labeled neurospheres to attach to astrocytes for 3 hr and then induced calcium waves by cutting into the monolayer. After 16 hr, neurospheres were dissociated, and DiI^+ cells were isolated by fluorescent activated cell sorting (FACS) and cultured at clonal density (1 cell/μL) (Figure 4C, schematic). After 10 days, the number and size of the spheres was analyzed. Sphere size indicates whether the founder cell was a stem cell or precursor cell (Louis et al., 2008). While the average sphere size showed no difference between the samples across the whole population, a comparison of the largest 2.4% of each sample, the approximate stem cell percentage in a neurosphere population (Reynolds and Rietze, 2005), revealed a significantly higher number of spheres with a diameter of >150 μm after injury compared with uninjured controls or thapsigargin-treated samples (Figures 4C [lower panel] and 4D). Equally, a higher capacity for self-renewal was observed based on the total number of spheres formed, with a significantly higher number after injury compared with the uninjured control or thapsigargin inhibition (Figure 4E). As an alternative way to increase intracellular calcium, we measured self-renewal of NSCs in the presence of 25 mM and 50 mM KCl, respectively. Both concentrations led to a decrease in self-renewal, indicating a different effect of an elevation of intracellular calcium by this method (Figure S3). Finally, we tested the effect of an astrocytic calcium wave on the differentiation capacity of NSCs. DiI-labeled neurospheres were allowed to attach on an astrocyte monolayer and then isolated after injury as described above. Calcium signaling was abolished for two experimental groups using thapsigargin and CPA, with addition of PBS serving as control. The isolated NSCs were then plated out on laminin-coated culture dishes under differentiating conditions, and after 3 days cell fates were examined by staining for GFAP and Tuj1. We did not observe any significant changes in the share of cell types generated between the different experimental groups (Figure 4F).

The Notch Signaling Pathway Mediates an Increase in Migratory Behavior of NSPCs

Notch signaling was found to play a role in multiple aspects of the reaction of NSPCs following stroke. To test the effect of calcium waves on Notch signaling in our experimental setup, we performed real-time qPCR analysis on mRNA

Figure 4. Calcium Signaling Increases Migratory and Self-Renewal Capacity of NSCs

(A and B) DiI-labeled neurospheres (outlined by green polygon) were placed on an astrocyte monolayer (asterisk indicates the injury cut; scale bar, 100 μm) (A) and the migration distances of individual cells were measured after 5 hr (B). For each of three independent experiments, the distance migrated by at least 70 cells was analyzed. Data represent mean ± SD. Statistical analysis by two-tailed unpaired t test: *$p < 0.05$; n.s., not significant.

(C) For self-renewal analysis, neurospheres were plated onto an astrocytic monolayer and 16 hr after injury the spheres were removed, dissociated to single cells, and replated at clonal density. Sphere size was measured after 10 days. For larger spheres reflecting a stem cell origin, sphere size was increased after injury but not in controls.

(D and E) The absolute number of spheres increased after injury (D) as well as that of larger spheres (E) compared with controls.

(F) Differentiation of neurosphere cells into a neuronal or glial lineage does not change after injury.

Data represent mean ± SD (n = 4 independent experiments in triplicate).

Statistical analysis by two-tailed unpaired t test: *$p < 0.05$; **$p < 0.01$; n.s., not significant.

extracted from neurospheres exposed to astrocytic calcium waves as described above. At various time intervals after injury, neurosphere cells were separated from astrocytes by FACS and RNA was isolated. Subsequent qPCR analysis demonstrated an upregulation of *Hes1*, an effector of Notch signaling, 30 min (Figure 5A) but not 1 hr, 4 hr, or 16 hr after injury. Other genes involved in the Notch signaling pathway, i.e., *Hes5*, *Notch1*, or the Notch1 ligand *Jagged1* were not upregulated. Notch signaling can be abolished by addition of DAPT (N-[N-(3,5-difluorophenacetyl)-L-alanyl]-S-phenylglycine t-butyl ester), an inhibitor of γ-secretase. γ-Secretase cleaves the Notch1 receptor and leads to the formation of the Notch intracellular domain, and is therefore necessary for functional Notch signaling. DAPT treatment of neurospheres led to a significant decrease in cell migration into the cell-free area of a scratch-wound assay, compared with the DMSO control (Figures 5B and 5C). Next, we investigated whether upregulated Notch1 signaling could also be induced in the SVZ of acute brain slices in a calcium-dependent manner. To this end, 250- to 300-μm thick vibratome slices of murine brains (postnatal days 10 and 11) were placed on a porous membrane and cultivated in a humidified atmosphere. After 2 days in culture, slices were treated either with CPA, an inhibitor of calcium-dependent ATPase, or with DMSO as a control. Subsequently, an injury was induced via transection of the slice, as illustrated in Figure 5D. The SVZs of the ipsilateral and contralateral hemispheres were harvested 3 or 24 hr after the injury for RNA isolation and subsequent qPCR analysis. Three hours after injury, *Hes1* and *Hes5* were upregulated in the ipsilateral compared with the contralateral SVZ, although *Hes5* upregulation was not significant (Figure 5E). However, in the CPA-treated samples the mRNA levels of both transcription factors remained unchanged compared with the contralateral DMSO control (Figure 5E). Notably, 24 hr after injury these effects could no longer be observed, as mRNA levels of *Hes1* and *Hes5* were unchanged in all samples (not shown).

DISCUSSION

In this study, we propose that astrocytic calcium waves are long-range signals capable of transmitting the occurrence of a brain injury to the SVZ, where they stimulate NSC proliferation and self-renewal and increase the migratory potential of NSPCs, as observed in various stroke models. Analysis of changes in gene expression in the SVZ after ischemia induced by a permanent occlusion of the middle cerebral artery showed a strong upregulation of components of the calcium-binding protein GO cluster, but not of signatures associated with immune cells or hypoxia. Given the typical properties of the SVZ reaction, in that it is fast and spatially limited to the injured hemisphere, we hypothesized that traveling astrocytic calcium waves arising from extensive tissue damage may transmit the information that a local injury has occurred over long distances to the SVZ. Interestingly, and similar to our findings, it was recently shown that calcium waves activate migratory behavior of microglia in the zebrafish brain in response to injury (Sieger et al., 2012). To study the effect of a physiological calcium signal carried only by astrocytes and transmitted to NSPCs in isolation, i.e., separated from simultaneously occurring processes such as neuronal transmission or spreading depression, we devised an in vitro co-culture system. NSCs can be very efficiently differentiated to astrocytes by addition of CNTF to the differentiation medium. A detailed characterization of calcium waves in these cells revealed a uniform propagating wave, recruiting all cells in a homogeneous fashion. Notably, the velocity of the astrocytic calcium waves of about 0.02 mm/s is three orders of magnitude slower compared with neuronal calcium waves, ranging between 30 and 50 mm/s (Stroh et al., 2013) and suggesting a differential mechanism of wave initiation and propagation. However, the velocity of these waves is in line with that of astrocytic calcium waves in the neocortex, at 0.014 ± 0.005 mm/s (Söhl et al., 2006). Also spreading depression, a form of neuronal slow propagation (3–6 mm/min, 0.05–0.1 mm/s) in rat cortex (Fujita et al., 2016) is accompanied by an astrocytic calcium wave (Peters et al., 2003). Central to our hypothesis, an elevation in intracellular calcium could be passed on from astrocytes to co-cultured neurospheres in vitro. We also observed the spreading of a calcium wave from the striatum to the adjacent SVZ in acute slices in vivo after electrical stimulation (Figure S4), showing kinetics similar to that of our in vitro data. In the astrocyte-neurosphere co-culture system we demonstrated an increase in sphere number, indicating increased self-renewal mediated by astrocytic calcium waves. Interestingly, we found a concomitant increase specifically in the population of the largest spheres. The largest spheres in a neurosphere culture typically arise from NSCs, in contrast to smaller spheres that originate in less primitive precursor cells or transient amplifying cells in vivo. Thus, the increase in the number of large spheres after a calcium signal may reflect a shift from asymmetric to symmetric division of stem cells, consistent with evidence from previous in vivo data (Zhang, 2004), rather than being the result of a simple change in proliferation that would affect all cells. Beyond this, calcium waves transmitted via gap junctions or by release of ATP and activation of purinergic receptors have been shown to influence neurogenesis in the adult brain SVZ (Lacar et al., 2011; Lin et al., 2007). The nature of the calcium signal to stem cells seems to be important for the type of response that is elicited. While NSC after astrocytic calcium wave did

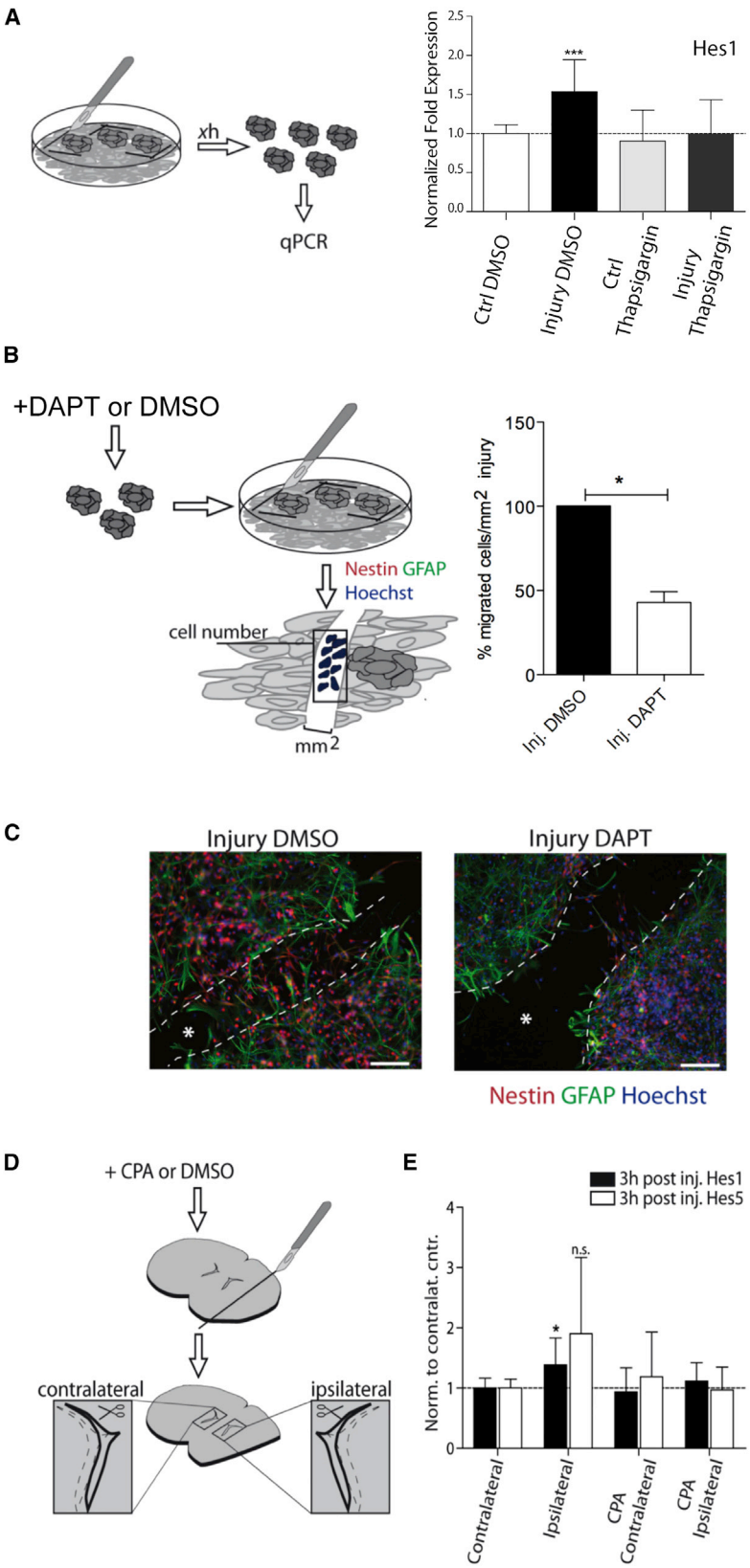

Figure 5. Calcium-Induced Changes Depend on Notch Signaling

(A) Neurosphere cells were isolated by FACS and analyzed by qPCR. *Hes1* was upregulated in neurospheres 30 min after injury (right panel).

(B) Left: schematic of the experiment. Neurospheres were treated with DAPT prior to the wound-scratch assay. The number of cells per mm^2 invading into the empty surface 16 hr after the injury was quantified after Hoechst staining. Right: DAPT treatment of the neurospheres decreased the number of cells that migrated into the cut after astrocytic injury.

(C) Examples of wound-scratch assays with DAPT-treated neurospheres. Cells that migrated into the scratch area were nestin positive. Asterisks indicate the injury cut. Scale bars, 50 μm.

(D) Brain slice cultures were treated either with CPA or DMSO as control. A part of the slice was cut away to induce an injury. SVZs were collected 3 hr later for RNA extraction.

(E) qPCR analysis of slice culture samples. Ipsilateral to the injury, *Hes1* and *Hes5* were upregulated, whereas in CPA-treated samples this effect was abolished.

Data were normalized to the contralateral DMSO control. For the qPCR, n = 4 independent experiments in triplicate and data represent mean ± SD. For the migration analysis, data represent mean ± SD. Statistical analysis by unpaired two-tailed t test: *p < 0.05, ***p < 0.001.

not change their differentiation potential, a previous study by one of the authors found that long-term optical stimulation of stem cells transduced with channelrhodopsin-2 led to an increase in neuronal differentiation and that this effect was likely due to calcium signaling (Stroh et al., 2011). In addition to initiating the injury response by an activation of quiescent NSCs, astrocytic calcium waves may have an important function in stimulating and guiding the migratory behavior of immature cells toward the injury. We showed that stimulating neurospheres with an astrocytic calcium wave was sufficient to increase cellular migratory potential. This was consistent with experiments showing that neurospheres cultivated from stroke mice display a higher migratory potential than that of neurospheres derived from non-stroke animals, indicating the induction of permanent changes (Zhang et al., 2007). The extent to which calcium signaling may contribute to directing neuroblast migration toward the injury site remains unclear, and a number of other signaling molecules have been suggested in this context. However, data on astrocytic calcium wave-induced responses in murine microglia (Schipke et al., 2002), as well as guidance of microglia in the zebrafish brain (Sieger et al., 2012), suggest that calcium waves are both necessary and sufficient for microglia migration to the site of injury.

The Notch signaling pathway is essential for maintaining embryonic NSCs and promoting gliogenesis. In stroke, it has been shown that molecules of the Notch signaling pathway are upregulated as little as 4 hr after MCAO (Wang et al., 2009b), indicating a role in the initiation of the injury reaction through the activation of stem cell proliferation. More recently, Notch signaling was demonstrated to convert ependymal cells directly into neuronal progenitor cells after stroke, thereby depleting the former and acting as a reservoir for additional progenitors (Carlén et al., 2009). Moreover, astrocytes could be induced to enter a neurogenic program in the striatum and medial cortex by blocking Notch signaling, even in the absence of stroke (Magnusson et al., 2014). These results point to a possibility of using endogenous neuronal differentiation potential for therapeutic strategies. Our results are consistent with an immediate activation of Notch signaling by an astrocytic calcium wave, measured by the upregulation of the Notch target gene *Hes1* in neurospheres or slice culture SVZs after injury, which could be reversed by blocking calcium signaling. Conversely, increased migration potential in neurospheres could be blocked by the γ-secretase inhibitor DAPT. From our data we cannot conclude that astrocytic calcium waves are the sole mediator of an injury response in vivo, and we find it likely that other factors or types of signaling contribute to the neurogenic injury response. For example, the attraction of stem cells transplanted into the contralateral hemisphere toward the lesion over a long distance would indicate other long-range signals (Hoehn et al., 2002). However, we give proof of concept that a transient increase in intracellular calcium levels can spread from astrocytes to NSPCs and that this signal is sufficient to increase their self-renewal and migratory behavior.

Conclusion

Our study adds to the general concept of calcium transients, initiated by distant events, regulating NSPC behavior in the SVZ. The confirmation of ongoing neurogenesis in the adult human brain, even in individuals of advanced age (Ernst and Frisén, 2015), gave a significant boost to the concept of using endogenous NSCs for brain repair. A better understanding of the signals that both activate and direct NSPCs from their niche to the site of injury is required for a further step toward this goal.

EXPERIMENTAL PROCEDURES

Stroke Model

Focal ischemia was induced by occlusion of the middle cerebral artery by electrocoagulation in adult male C57/BL6 mice (7–8 weeks old; Charles River). All animal work was conducted according to the relevant institutional guidelines of the Frankfurt University Medical School and was approved by the government agency for veterinary medicine in Darmstadt, Germany (ethical permission Gen. Nr. F94/12; F94/09; F 31/15). Sham surgery was used in control animals, performing the same procedure except for occlusion of the artery. Forty-eight hours after MCAO the mice were killed, the brains removed, and the SVZ rapidly excised in ice-cold PBS and collected in RNAlater (Life Technologies). Only animals with tissue damage not extended to the SVZ were included in further analysis.

Affymetrix Microarray Analysis

RNA quality was checked using the Bioanalyzer (Agilent Technologies) RNA 6000 Pico LabChip Kit. Five micrograms of RNA was used for hybridization for each sample on a GeneChip Mouse Genome 430 2.0 array (Affymetrix). Probe level normalization was conducted using the variance stabilization method (Huber et al., 2002). This method renders the variance of probe intensities approximately independent of their expected expression levels. Parameters (offset and a scaling factor) were estimated for each microarray, in consideration of the fact that a reasonable fraction of probes was not differentially expressed across the samples. In view of the computational complexity of the algorithm, parameters were estimated from a random subset of probes and then used to transform the complete arrays. Probeset summarization was calculated using the median polish method on the normalized data. For each probeset a robust additive model was fitted across the arrays, addressing the different sensitivity of the probesets via the probe effect. Firstly, an expression intensity filter was used to reduce the dimension of the microarray data. Data were filtered with an intensity filter (the intensity of a gene should be higher than 100 in at least 0.25% of samples, if the group size is

equal) and a variance filter (the interquartile range of $\log_2$ intensities should be at least 0.5, if the group size is equal). After the expression intensity filtering, we calculated p values with the two-sample t test (variance = equal) to identify genes that were differentially expressed between the two groups. For the multiple testing problems, we used a false discovery rate (FDR). Furthermore, fold changes (FC) between the two groups were calculated for each gene. The lists of differentially expressed genes were filtered with FDR and FC criteria. A heatmap was generated with Spotfire Software (Spotfire Decision Site 9.1.2).

Cell Culture and Reagents

Primary neurospheres were cultivated from the brains of adult male C57Bl/6 mice as described previously (Johansson et al., 1999). For astrocytic monolayer differentiation, cell-culture plates were coated with poly-L-lysine solution in PBS for at least 1 hr prior to cell cultivation. After dissociation, neurosphere cells were counted and plated into coated dishes containing differentiation medium with 1 μM CNTF for at least 2 days prior to calcium signaling experiments. For fluorescent staining of neurospheres, cells were incubated in culture medium containing 2 μM DiI (Molecular Probes) at 37°C for 5 min followed by 15 min at 4°C. Afterward, cells were washed twice with DMEM to remove excess dye.

Fluorescence-Activated Cell Sorting

Astrocyte-neurosphere co-cultures were briefly washed with cold PBS. For cell detachment, co-cultures were incubated with Accutase for 5–10 min until cells were completely dissociated to single cells. Cells were washed once with medium and then resuspended in PBS-HEPES solution, and kept on ice previous to sorting. Sorting was performed on a FACSAria (Becton Dickinson). For self-renewal analysis, cells were sorted directly into 6-well plates at a clonal density of 1 cell/μL in culture medium. For RNA isolation, cells were sorted into RNase/DNase-free tubes. Approximately 100,000 cells were sorted for each condition. Immediately after sorting, cells were centrifuged and the resulting pellet was resuspended in lysis buffer for RNA isolation.

Brain Slice Cultures and Analysis

Brain slices were prepared from mice from postnatal days 6 to 14. Mice were killed by cervical dislocation and the brains were excised, washed briefly in ice-cold Krebs buffer, and embedded in low melting agarose in plastic embedding molds. Slices were cut at 250–300 μm thickness and placed into ice-cold Krebs buffer saturated with carbogen. Brain slices were transferred onto porous polycarbonate membrane and cultivated in a humidified atmosphere in serum-containing medium for 2 hr. Afterward, the medium was changed to neurosphere culture medium and replaced every day thereafter. For analysis of gene expression in the SVZ, 50 μM CPA was added to the slice culture medium to inhibit calcium signaling. After 45 min of incubation, an injury was induced by cutting into the slice with a blade. SVZs were dissected out 3 hr or 24 hr afterward and immediately placed in lysis buffer for RNA extraction and analysis.

Calcium Imaging In Vitro

For calcium imaging of both astrocytes and neurospheres, spheres were allowed to attach to the astrocytic monolayer for at least 2 hr prior to staining. Cell cultures were stained with either 5 μM Fluo-4AM or 10 μM OGB1, both diluted in culture medium, for 45 min at 37°C in humidified atmosphere. After the incubation time, cells were washed with warm culture media and analyzed within 2 hr. Drugs were applied via bath application. All drugs were applied for 30 min, except carbenoxolone, which was applied 5 min before analysis. An injury of the astrocytic monolayer was induced by either cutting with a blade or scratching with the tip of a 10-μL pipette. Cells stained with Fluo4-AM were analyzed under a confocal microscope with a frequency of 1 Hz; cells stained with OGB1 were analyzed under a fluorescent microscope with a frequency of >18 Hz. For imaging of astrocyte-neurosphere co-cultures, neurospheres were labeled with the red fluorescent dye DiI (Invitrogen) prior to attachment to the astrocytic monolayer.

Calcium Wave Analysis

First, we defined regions of interest (ROIs) semi-automatically and fitted a line to the site of mechanical lesion. Next, we calculated the minimum distance to each ROI center of mass to the linear lesion and sorted the ROIs according to those values. We examined the correlation between the time to peak normalized fluorescence ($\Delta F/F$) and the distance from the lesion. We fitted a line using the least-square method. The amount of variance explained by the linear fit was determined by linear regression using the aforementioned parameters with distance from the lesion as predictor. Finally, the velocity of the calcium wave was obtained from the inverse of the slope of the best-fitting line to the latter relationship. Heatmaps were constructed with the sorted matrices described above. All calculations were performed in MATLAB (MathWorks).

Calcium Imaging of Brain Slices

After preparation, brain slices were transferred onto a nylon grid in artificial cerebrospinal fluid (ACSF) buffer, continuously saturated with carbogen, and loaded with the calcium indicator dye Fluo4-AM (10 μM) for 45 min at room temperature with constant carbogen perfusion. Electrical stimulation and induction of calcium waves was performed as described previously (Schipke et al., 2002). In brief, slices were transferred to a perfusion chamber and fixed by using a U-shaped platinum wire with a grid of nylon threads. Slices were continuously perfused with carbogen at a constant flow of 5 mL/min. All experiments were performed at 34°C. Intracellular calcium changes were detected with a sampling rate of 1 Hz. Electrical stimulation was accomplished with a glass electrode filled with ACSF solution. The pipettes had a resistance of ≈1 MΩ, which corresponds to a tip opening of ≈15 μm. The tip of the pipette was placed outside the SVZ, at the top of the slice. After the positioning of the pipette the slice was allowed to recover from mechanical stress for at least 2 min. The wave was elicited by applying 10-Hz stimulation for 4 s at 30 μA. The pulses were generated by a patch-clamp amplifier and isolated using a stimulus isolator. The calcium wave could be triggered repetitively within the same area, allowing the time between stimulations of at least 5 min.

RNA Isolation and Analysis

For RNA isolation, cells were sorted in DNase/RNase-free collection tubes. Cell numbers of sorted cells were similar for all conditions within a single experiment (between 50,000 and 200,000 cells).

Cells were centrifuged immediately and a volume of 350 μL of RLTplus buffer containing additional β-mercaptoethanol (10 μL/mL) was added. RNA was isolated using an RNeasy mini kit according to the manufacturer's protocol and reverse transcribed with the High-Capacity RNA to cDNA kit (Applied Biosystems) according to the manufacturer's instructions. qPCR was performed on a MyiQ iCycler (Bio-Rad) using either SYBR Green System (Bio-Rad) for cells or TaqMan System (Thermo Fisher Scientific) for slices, in triplicates, according to the manufacturer's protocol. *Rpl13a* and *Sdha* housekeeping genes were used as controls: 5 ng cDNA were used for each sample.

Fluorescence Immunohistochemistry

Cryostat brain sections (15 μm) were incubated with primary antibody diluted in 10% normal goat serum and 0.1% Triton X-100 in PBS at 4°C overnight. The next day, sections were washed with PBS three times and incubated with secondary antibody, and diluted in PBS for 45 min at room temperature. Following incubation, brain sections were washed and embedded with AquaPolyMount medium. Fluorescent images were captured on a confocal LSM Nikon TE2000-E microscope. Images were processed using EC-C1 3.60 software and ImageJ (NIH). The following antibodies were used: monoclonal mouse anti-GFAP (1:500; Millipore MAB5804); polyclonal rabbit anti-GFAP (1:1,000; Dako Z0334); monoclonal mouse anti-human CD45/leukocyte common antigen (1:50; Dako MO701); monoclonal mouse anti-human nestin (1:200; Millipore MAB5326); and polyclonal rabbit anti-Iba1 (Wako Pure Chemical Industries 019-19741).

ACCESSION NUMBERS

The data discussed in this publication have been deposited in the NCBI GEO (Edgar et al., 2002) and are accessible through NCBI GEO: GSE93376.

SUPPLEMENTAL INFORMATION

Supplemental Information includes four figures and can be found with this article online at http://dx.doi.org/10.1016/j.stemcr.2017.01.009.

AUTHOR CONTRIBUTIONS

A.K., E.R.J., conception and design, collection and/or assembly of data, and data analysis and interpretation; A.R., R.v.L., M.G., collection and/or assembly of data; C.D., data analysis and interpretation; M.Z., conception and design and administrative support; H.K., conception and design, data analysis and interpretation; A.S., conception and design, data analysis and interpretation, and manuscript writing; S.M., conception and design, collection and/or assembly of data, data analysis and interpretation, manuscript writing, and final approval of manuscript.

ACKNOWLEDGMENTS

This study was supported by the Edinger Foundation; A.K. was a MainCampus scholar. Affymetrix GeneChip hybridizations were performed at Chip Facility, Interdisciplinary Center for Clinical Research (IZKF) Aachen, RWTH Aachen University, Aachen, Germany.

Received: January 8, 2016
Revised: January 12, 2017
Accepted: January 12, 2017
Published: February 16, 2017

REFERENCES

Arvidsson, A., Collin, T., Kirik, D., Kokaia, Z., and Lindvall, O. (2002). Neuronal replacement from endogenous precursors in the adult brain after stroke. Nat. Med. *8*, 963–970.

Boitano, S., Dirksen, E.R., and Sanderson, M.J. (1992). Intercellular propagation of calcium waves mediated by inositol trisphosphate. Science *258*, 292–295.

Carlén, M., Meletis, K., Göritz, C., Darsalia, V., Evergren, E., Tanigaki, K., Amendola, M., Barnabé-Heider, F., Yeung, M.S.Y., Naldini, L., et al. (2009). Forebrain ependymal cells are Notch-dependent and generate neuroblasts and astrocytes after stroke. Nat. Neurosci. *12*, 259–267.

Chirasani, S.R., Sternjak, A., Wend, P., Momma, S., Campos, B., Herrmann, I.M., Graf, D., Mitsiadis, T., Herold-Mende, C., Besser, D., et al. (2010). Bone morphogenetic protein-7 release from endogenous neural precursor cells suppresses the tumourigenicity of stem-like glioblastoma cells. Brain *133*, 1961–1972.

Cotrina, M.L., Lin, J.H., Alves-Rodrigues, A., Liu, S., Li, J., Azmi-Ghadimi, H., Kang, J., Naus, C.C., and Nedergaard, M. (1998). Connexins regulate calcium signaling by controlling ATP release. Proc. Natl. Acad. Sci. USA *95*, 15735–15740.

Crespel, A., Rigau, V., Coubes, P., Rousset, M.C., de Bock, F., Okano, H., Baldy-Moulinier, M., Bockaert, J., and Lerner-Natoli, M. (2005). Increased number of neural progenitors in human temporal lobe epilepsy. Neurobiol. Dis. *19*, 436–450.

Curtis, M.A., Penney, E.B., Pearson, A.G., van Roon-Mom, W.M.C., Butterworth, N.J., Dragunow, M., Connor, B., and Faull, R.L.M. (2003). Increased cell proliferation and neurogenesis in the adult human Huntington's disease brain. Proc. Natl. Acad. Sci. USA *100*, 9023–9027.

Edgar, R., Domrachev, M., and Lash, A.E. (2002). Gene Expression Omnibus: NCBI gene expression and hybridization array data repository. Nucleic Acids Res. *30*, 207–210.

Ernst, A., and Frisén, J. (2015). Adult neurogenesis in humans—common and unique traits in mammals. PLoS Biol. *13*, e1002045.

Ernst, A., Alkass, K., Bernard, S., Salehpour, M., Perl, S., Tisdale, J., Possnert, G., Druid, H., and Frisén, J. (2014). Neurogenesis in the striatum of the adult human brain. Cell *156*, 1072–1083.

Felling, R.J., Snyder, M.J., Romanko, M.J., Rothstein, R.P., Ziegler, A.N., Yang, Z., Givogri, M.I., Bongarzone, E.R., and Levison, S.W. (2006). Neural stem/progenitor cells participate in the regenerative response to perinatal hypoxia/ischemia. J. Neurosci. *26*, 4359–4369.

Fujita, S., Mizoguchi, N., Aoki, R., Cui, Y., Koshikawa, N., and Kobayashi, M. (2016). Cytoarchitecture-dependent decrease in propagation velocity of cortical spreading depression in the rat insular cortex revealed by optical imaging. Cereb. Cortex *26*, 1580–1589.

Glass, R., Synowitz, M., Kronenberg, G., Walzlein, J., Walzlein, J.-H., Markovic, D.S., Wang, L.-P., Wang, L., Gast, D., Kiwit, J., et al. (2005). Glioblastoma-induced attraction of endogenous neural precursor cells is associated with improved survival. J. Neurosci. *25*, 2637–2646.

Guthrie, P.B., Knappenberger, J., Segal, M., Bennett, M.V., Charles, A.C., and Kater, S.B. (1999). ATP released from astrocytes mediates glial calcium waves. J. Neurosci. *19*, 520–528.

Hoehn, M., Küstermann, E., Blunk, J., Wiedermann, D., Trapp, T., Wecker, S., Föcking, M., Arnold, H., Hescheler, J., Fleischmann, B.K., et al. (2002). Monitoring of implanted stem cell migration in vivo: a highly resolved in vivo magnetic resonance imaging investigation of experimental stroke in rat. Proc. Natl. Acad. Sci. USA *99*, 16267–16272.

Huber, W., von Heydebreck, A., Sültmann, H., Poustka, A., and Vingron, M. (2002). Variance stabilization applied to microarray data calibration and to the quantification of differential expression. Bioinformatics *18* (*Suppl 1*), S96–S104.

Imitola, J., Raddassi, K., Park, K.I., Mueller, F.J., Nieto, M., Teng, Y.D., Frenkel, D., Li, J., Sidman, R.L., Walsh, C.A., et al. (2004). Directed migration of neural stem cells to sites of CNS injury by the stromal cell-derived factor 1alpha/CXC chemokine receptor 4 pathway. Proc. Natl. Acad. Sci. USA *101*, 18117–18122.

Jin, K., Wang, X., Xie, L., Mao, X.O., Zhu, W., Wang, Y., Shen, J., Mao, Y., Banwait, S., and Greenberg, D.A. (2006). Evidence for stroke-induced neurogenesis in the human brain. Proc. Natl. Acad. Sci. USA *103*, 13198–13202.

Johansson, C.B., Momma, S., Clarke, D.L., Risling, M., Lendahl, U., and Frisén, J. (1999). Identification of a neural stem cell in the adult mammalian central nervous system. Cell *96*, 25–34.

Johe, K.K., Hazel, T.G., Muller, T., Dugich-Djordjevic, M.M., and McKay, R.D.G. (1996). Single factors direct the differentiation of stem cells from the fetal and adult central nervous system. Genes Dev. *10*, 3129–3140.

Kawai, T., Takagi, N., Nakahara, M., and Takeo, S. (2005). Changes in the expression of Hes5 and Mash1 mRNA in the adult rat dentate gyrus after transient forebrain ischemia. Neurosci. Lett. *380*, 17–20.

Lacar, B., Young, S.Z., Platel, J.-C., and Bordey, A. (2011). Gap junction-mediated calcium waves define communication networks among murine postnatal neural progenitor cells. Eur. J. Neurosci. *34*, 1895–1905.

Lacar, B., Herman, P., Platel, J.C., Kubera, C., Hyder, F., and Bordey, A. (2012). Neural progenitor cells regulate capillary blood flow in the postnatal subventricular zone. J. Neurosci. *32*, 16435–16448.

Lin, J.H.-C., Takano, T., Arcuino, G., Wang, X., Hu, F., Darzynkiewicz, Z., Nunes, M., Goldman, S.A., and Nedergaard, M. (2007). Purinergic signaling regulates neural progenitor cell expansion and neurogenesis. Dev. Biol. *302*, 356–366.

Lindvall, O., and Kokaia, Z. (2006). Stem cells for the treatment of neurological disorders. Nature *441*, 1094–1096.

Louis, S.A., Rietze, R.L., Deleyrolle, L., Wagey, R.E., Thomas, T.E., Eaves, A.C., and Reynolds, B.A. (2008). Enumeration of neural stem and progenitor cells in the neural colony-forming cell assay. Stem Cells *26*, 988–996.

Macas, J., Nern, C., Plate, K.H., and Momma, S. (2006). Increased generation of neuronal progenitors after ischemic injury in the aged adult human forebrain. J. Neurosci. *26*, 13114–13119.

Macas, J., Ku, M.-C., Nern, C., Xu, Y., Bühler, H., Remke, M., Synowitz, M., Franz, K., Seifert, V., Plate, K.H., et al. (2014). Generation of neuronal progenitor cells in response to tumors in the human brain. Stem Cells *32*, 244–257.

Magnusson, J.P., Göritz, C., Tatarishvili, J., Dias, D.O., Smith, E.M.K., Lindvall, O., Kokaia, Z., and Frisén, J. (2014). A latent neurogenic program in astrocytes regulated by Notch signaling in the mouse. Science *346*, 237–241.

Owens, D.F., and Kriegstein, A.R. (1998). Patterns of intracellular calcium fluctuation in precursor cells of the neocortical ventricular zone. J. Neurosci. *18*, 5374–5388.

Peters, O., Schipke, C.G., Hashimoto, Y., and Kettenmann, H. (2003). Different mechanisms promote astrocyte Ca^{2+} waves and spreading depression in the mouse neocortex. J. Neurosci. *23*, 9888–9896.

Reynolds, B.A., and Rietze, R.L. (2005). Neural stem cells and neurospheres—re-evaluating the relationship. Nat. Methods *2*, 333–336.

Scemes, E., and Giaume, C. (2006). Astrocyte calcium waves: what they are and what they do. Glia *54*, 716–725.

Schipke, C.G., Boucsein, C., Ohlemeyer, C., Kirchhoff, F., and Kettenmann, H. (2002). Astrocyte Ca^{2+} waves trigger responses in microglial cells in brain slices. FASEB J. *16*, 255–257.

Sieger, D., Moritz, C., Ziegenhals, T., Prykhozhij, S., and Peri, F. (2012). Long-range Ca^{2+} waves transmit brain-damage signals to microglia. Dev. Cell *22*, 1138–1148.

Söhl, G., Willecke, K., Haas, B., Kettenmann, H., Schipke, C.G., and Peters, O. (2006). Activity-dependent ATP-waves in the mouse neocortex are independent from astrocytic calcium waves. Cereb. Cortex *16*, 237–246.

Spalding, K.L., Bergmann, O., Alkass, K., Bernard, S., Salehpour, M., Huttner, H.B., Boström, E., Westerlund, I., Vial, C., Buchholz, B.A., et al. (2013). Dynamics of hippocampal neurogenesis in adult humans. Cell *153*, 1219–1227.

Stroh, A., Tsai, H.C., Wang, L.P., Zhang, F., Kressel, J., Aravanis, A., Santhanam, N., Deisseroth, K., Konnerth, A., and Schneider, M.B. (2011). Tracking stem cell differentiation in the setting of automated optogenetic stimulation. Stem Cells *29*, 78–88.

Stroh, A., Adelsberger, H., Groh, A., Rühlmann, C., Fischer, S., Schierloh, A., Deisseroth, K., and Konnerth, A. (2013). Making waves: initiation and propagation of corticothalamic Ca^{2+} waves in vivo. Neuron *77*, 1136–1150.

Takasawa, K., Kitagawa, K., Yagita, Y., Sasaki, T., Tanaka, S., Matsushita, K., Ohstuki, T., Miyata, T., Okano, H., Hori, M., et al. (2002). Increased proliferation of neural progenitor cells but reduced survival of newborn cells in the contralateral hippocampus after focal cerebral ischemia in rats. J. Cereb. Blood Flow Metab. *22*, 299–307.

Wang, L., Chopp, M., Zhang, R.L., Zhang, L., LeTourneau, Y., Feng, Y.F., Jiang, A., Morris, D.C., and Zhang, Z.G. (2009a). The Notch pathway mediates expansion of a progenitor pool and neuronal

differentiation in adult neural progenitor cells after stroke. Neuroscience *158*, 1356–1363.

Wang, X., Mao, X., Xie, L., Greenberg, D.A., and Jin, K. (2009b). Involvement of Notch1 signaling in neurogenesis in the subventricular zone of normal and ischemic rat brain in vivo. J. Cereb. Blood Flow Metab. *29*, 1644–1654.

Zhang, R. (2004). Stroke transiently increases subventricular zone cell division from asymmetric to symmetric and increases neuronal differentiation in the adult rat. J. Neurosci. *24*, 5810–5815.

Zhang, R.L., LeTourneau, Y., Gregg, S.R., Wang, Y., Toh, Y., Robin, A.M., Zhang, Z.G., and Chopp, M. (2007). Neuroblast division during migration toward the ischemic striatum: a study of dynamic migratory and proliferative characteristics of neuroblasts from the subventricular zone. J. Neurosci. *27*, 3157–3162.